A Single Test Protocol to Establish the Full Spectrum of Exercise Intensity Prescription

DANILO IANNETTA[1], MARY Z. MACKIE[1], DANIEL A. KEIR[2], and JUAN M. MURIAS[1,3]

[1]Faculty of Kinesiology, University of Calgary, Calgary, AB, CANADA; [2]School of Kinesiology, Western University, London, ON, CANADA; and [3]College of Health and Life Sciences, Hamad Bin Khalifa University, Doha, QATAR

ABSTRACT

IANNETTA, D., M. Z. MACKIE, D. A. KEIR, and J. M. MURIAS. A Single Test Protocol to Establish the Full Spectrum of Exercise Intensity Prescription. *Med. Sci. Sports Exerc.*, Vol. 55, No. 12, pp. 2271–2280, 2023. Via the identification of the ramp-specific gas exchange threshold (GET) and respiratory compensation point (RCP), the recently validated step–ramp–step (SRS) protocol enables the prediction of the power outputs at the lactate threshold and maximal metabolic steady state. **Purpose:** We aimed to test the extended capabilities of the SRS protocol by validating its capacity to predict the power outputs for targeted metabolic rates ($\dot{V}O_2$) and time-to-task failure (T_{lim}) within the heavy- and severe-intensity domain, respectively. **Methods:** Fourteen young individuals completed (i) an SRS protocol from which the power outputs at GET and RCP (RCP_{CORR}), and the work accruable above RCP_{CORR}, defined as W'_{RAMP}, were derived; (ii) one heavy-intensity bout at a power output predicted to elicit a targeted $\dot{V}O_2$ equidistant from GET and RCP; and (iii) four severe-intensity trials at power outputs predicted to elicit targeted T_{lim} at minutes 2.5, 5, 10, and 13. These severe-intensity trials were also used to compute the constant-load–derived critical power and W' ($W'_{CONSTANT}$). **Results:** Targeted (2.41 ± 0.52 L·min^{-1}) and measured (2.43 ± 0.52 L·min^{-1}) $\dot{V}O_2$ at the identified heavy-intensity power output (162 ± 43 W) were not different ($P = 0.71$) and substantially concordant (CCC = 0.95). Likewise, targeted and measured T_{lim} for the four identified severe-intensity power outputs were not different ($P > 0.05$), and the aggregated coefficient of variation was 10.7% ± 8.9%. The derived power outputs at RCP_{CORR} (192 ± 53 W) and critical power (193 ± 53 W) were not different ($P = 0.65$) and highly concordant (CCC = 0.99). There were also no differences between W'_{RAMP} and $W'_{CONSTANT}$ ($P = 0.51$). **Conclusions:** The SRS protocol can accurately predict power outputs to elicit discrete metabolic rates and exercise durations, thus providing, with time efficiency, a high precision for the control of the metabolic stimulus during exercise. **Key Words:** MAXIMAL METABOLIC STEADY STATE, LACTATE THRESHOLD, CRITICAL POWER, EXERCISE INTENSITY DOMAINS

When prescribing intensity for constant-load exercise, the probabilities of inducing the desired metabolic stimulus are highest if the external load (e.g., power output) is assigned in relation to two distinct metabolic boundaries: the lactate threshold (LT) and the maximal metabolic steady state (MMSS) (1), respectively occurring within the range of ~55%–60% and ~75%–90% of an individual's maximal O_2 consumption ($\dot{V}O_{2max}$). Indeed, the position of these boundaries in relation to $\dot{V}O_{2max}$ dictates whether a given power output can be sustained in steady state with minimal (if <LT, moderate-intensity domain) or heightened but stable (if >LT but <MMSS, heavy-intensity domain) metabolic perturbations, or whether it cannot be sustained in steady state because of the continuous deterioration of muscle contractile efficiency (if >MMSS, severe-intensity domain) (2). As such, developing accurate, simple, and time-efficient strategies to identify the external load associated with these boundaries is key to maximize the effectiveness of any exercise-based intervention.

In line with the goal of facilitating the prediction of the power output at LT and MMSS, we recently developed a novel, single-visit exercise test protocol that consists of adding one moderate-intensity (before) and one heavy-intensity (after) step transition to a standard ramp-incremental test (3). The performance of these step transitions aids with the reconstruction of the $\dot{V}O_2$-to-power output relationship, which becomes increasingly misaligned during rapidly incrementing ramp protocols by the progressive slowing of the $\dot{V}O_2$ kinetics (4,5). Upon the alignment of the $\dot{V}O_2$-to-power output relationship, this step–ramp–step (SRS) protocol permits the prediction of the power output at LT and MMSS via linear interpolation of the $\dot{V}O_2$ at the gas exchange threshold (GET) and at the respiratory compensation point (RCP) (3), which are the ramp-specific manifestations of LT and MMSS (6). Although there is some debate as to whether RCP can be used to derive MMSS (7–14), when testing the validity of the SRS protocol, we found, as hypothesized, that cycling at the "corrected" power output at RCP (RCP_{CORR}) elicited physiological responses conforming to heavy-intensity exercise (i.e., stable

Address for correspondence: Juan M. Murias, Ph.D., College of Health and Life Sciences, Hamad Bin Khalifa University, 2D21 GU Building, Doha, Qatar; E-mail: jmurias@hbku.edu.qa.
Submitted for publication March 2023.
Accepted for publication June 2023.

0195-9131/23/5512-2271/0
MEDICINE & SCIENCE IN SPORTS & EXERCISE®

DOI: 10.1249/MSS.0000000000003249

$\dot{V}O_2$ and blood lactate concentration ($[La^-]_b$), whereas cycling 5% above this power output was associated with responses typical of severe-intensity exercise (i.e., inability to to complete the task and/or unstable). Because these divergent responses were elicited with the smallest deviation in power output (i.e., 5%) from RCP_{CORR} in most of the individuals, such results demonstrated the ability of the SRS protocol to locate with good accuracy the power outputs delimitating the exercise intensity domains.

Still, the SRS protocol has the potential to further improve the quality of exercise intensity prescription when using data derived from ramp-incremental tests. First, although the protocol was specifically designed to predict the power outputs yielding, in steady state, the $\dot{V}O_2$ at GET/LT and RCP/MMSS, the approximate linearity of the increase in $\dot{V}O_2$ gain from GET to RCP (5) would suggest the possibility of predicting the power output for any target $\dot{V}O_2$ within the heavy-intensity domain. Second, presuming that the power output at RCP_{CORR} would occur in close proximity to the power output at critical power (CP)—an operational surrogate of MMSS (3)—the SRS protocol could also enable the prediction of power outputs for any target time-to-task failure (T_{lim}) within the severe-intensity domain. Indeed, although presenting some variability when it comes to ramped exercise (12,15), it is well established that the work (J) that can be accrued above CP, defined as W', appears to be restricted to a finite amount irrespective of the exercise paradigm used (16,17). Thus, assuming that RCP_{CORR} is not different from CP and that at the end of the ramp-incremental exercise W' is fully depleted (17), the finite amount of work performed above RCP_{CORR} can be calculated (16) and, theoretically, be used to predict the power output for any target T_{lim} within the severe-intensity domain.

Therefore, we used the SRS protocol to test the hypotheses that it would be capable of predicting the power outputs that would elicit target (i) $\dot{V}O_2$ within the heavy-intensity domain and (ii) T_{lim} within the severe-intensity domain. To further corroborate its methodological robustness, we also tested the hypothesis that the ramp-derived RCP_{CORR} and W' (W'_{RAMP}) would not be different from the constant-load–derived CP and W' ($W'_{CONSTANT}$). If these hypotheses are proven correct, the SRS protocol would represent the only single-visit test protocol capable of predicting power outputs for target metabolic rates and exercise performance across the entire intensity spectrum.

METHODS

Fourteen individuals [nine males (age = 32 ± 9 yr, stature = 180 ± 7 cm, body mass = 75 ± 11 kg) and five females (age = 23 ± 3 yr, stature = 166 ± 7 cm, body mass = 63 ± 12 kg) gave their written consent and participated in the study, which was approved by the Conjoint Health Research Ethics Board of the University of Calgary. All the procedures relative to this study conformed to the standards established by the latest version of the Declaration of Helsinki. All participants were healthy, nonsmokers, and not taking medications that could alter their metabolic and cardiorespiratory responses to exercise.

Exercise Protocols

A schematic representation of the research design is depicted in Figure 1. Participants visited the laboratory on eight to nine occasions. The first visit consisted of performance of the SRS protocol. Upon the estimation of the $\dot{V}O_2$ and "corrected" power outputs at GET and RCP (3), during the following visits participants completed (i) two to three 30-min, constant-load trials to confirm MMSS based on the RCP_{CORR}; (ii) one 12-min, constant-load trial at a predetermined power output within the heavy-intensity domain; and (iii) four constant-load trials to task failure at predetermined power outputs within the severe-intensity domain. Each visit was completed at the same time of the day (±30 min) and separated by at least 48 h. During the first visit, participants were asked to cycle at their preferred cadence within the range of 75–95 rpm. This cadence was then recorded and used for all subsequent visits. For the ramp phase of the SRS protocol and for all the constant-load severe-intensity trials, T_{lim} was determined as the inability to continue the task and/or to maintain the self-selected cadence for more than 10 s despite strong verbal encouragement.

SRS protocol. The SRS protocol consisted of (i) one moderate-intensity step transition, (ii) one ramp-incremental test, and (iii) one heavy-intensity step transition. Based on the target population being recruited (recreationally active), we selected 80 W for the moderate-intensity step transition. For each participant, confirmation that this power output resided within the moderate-intensity domain was done *a posteriori*. The transition was initiated after a baseline cycling of 2 min at 20 W and sustained for 6 min. Thereafter, a 4-min baseline at 20 W preceded the ramp-incremental test, which was set at a

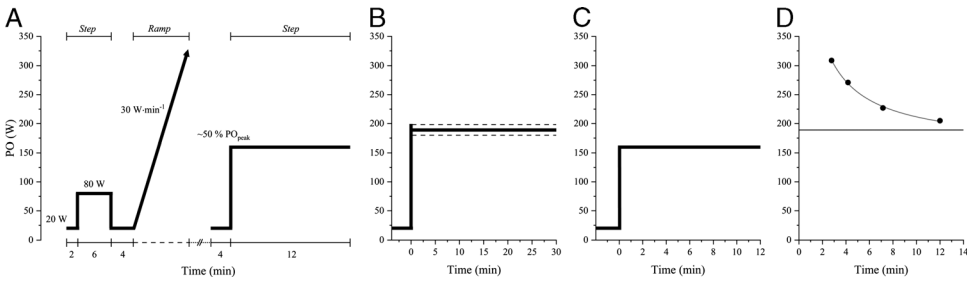

FIGURE 1—Schematic representation of the research design. On the performance of the SRS protocol on their first visit (A), on subsequent visits participants performed two to three 30-min constant-load trials to confirm MMSS from RCP_{CORR} (B), one heavy-intensity step transition to at $HVY_{50\%}$ (C), and four severe-intensity constant-load trials at power outputs predicted to elicit failure at minutes 2.5, 5, 10, and 13.

rate of 30 W·min^{-1}. Approximately 30 min after completion of the ramp-incremental test, the 12-min, heavy-intensity step transition was performed at a power output of 45%–60% of the peak power output (PO_{peak}) attained during the ramp test (18). The ramp-derived gas exchange and ventilatory data were visually scrutinized during the 30-min break to ensure that the selected heavy-intensity power output would elicit a $\dot{V}O_2$ appreciably higher than the one estimated at GET but below the one estimated at RCP (3).

Constant-load trials for RCP_{CORR} confirmation. Starting from the power output at RCP_{CORR}, on different days participants performed two to three 30-min constant-load trials to characterize the MMSS. Depending on whether the $\dot{V}O_2$ and the $[La^-]_b$ responses were considered stable, and whether participants could complete the 30-min trials, the power output for the subsequent trial was either increased or decreased by 5% from the power output at RCP_{CORR}. A steady-state $\dot{V}O_2$ response was established when the end-trial $\dot{V}O_2$ was ≤95% of $\dot{V}O_{2max}$ and/or if changes from minute 20 to minute 30 were ≤120 mL·min^{-1}. By contrast, a steady-state $[La^-]_b$ response was established when, for the same time interval, changes in $[La^-]_b$ were ≤1 mM (19).

Heavy-intensity constant-load trial. To test the predictive ability of the SRS protocol within the heavy-intensity domain, participants were asked to complete a 12-min trial at a power output that would elicit a $\dot{V}O_2$ response falling midway between the $\dot{V}O_2$ at GET and RCP ($HVY_{50\%}$). This power output was selected from the linear extrapolation of the $\dot{V}O_2$-to-power output relationship between these two indices (for details, see Data Analyses section). For instance, as shown in Figure 2, for a representative participant, if the $\dot{V}O_2$ at GET and RCP were estimated, respectively, at 2.80 and 3.95 L·min^{-1}, then the power output was linearly extrapolated to elicit a target $\dot{V}O_2$ of 3.38 L·min^{-1}.

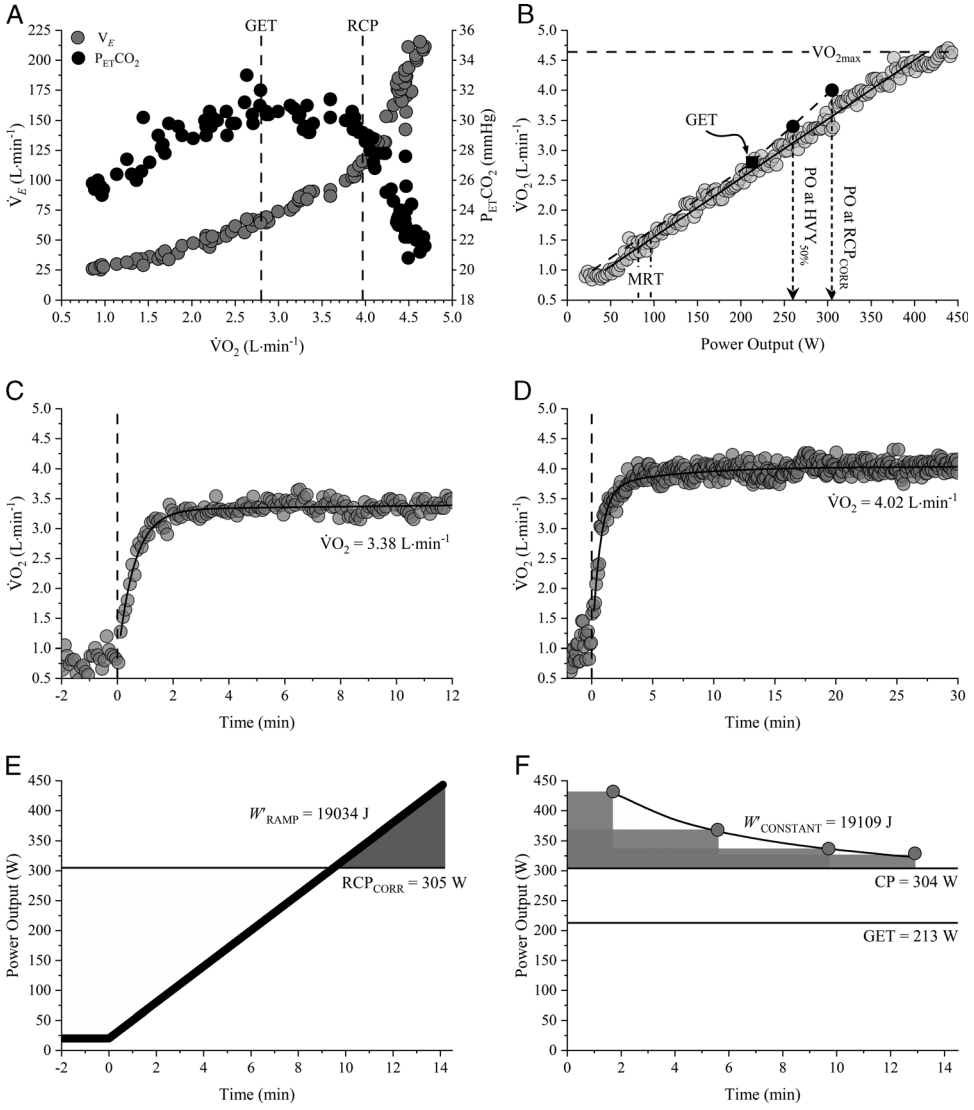

FIGURE 2—Profiles for a representative participant. A, The identification of GET and RCP during the ramp phase of the SRS protocol. B, The correction applied to the ramp $\dot{V}O_2$ data according to the outcomes of the SRS protocol. C, D, The $\dot{V}O_2$ responses for $HVY_{50\%}$ and RCP_{CORR}. E, F, The power output at RCP_{CORR} and CP and the derived W'_{RAMP} and $W'_{CONSTANT}$.

Severe-intensity constant-load trials. To tests the predictive ability of the SRS protocol within the severe-intensity domain, participants performed four severe-intensity constant-load trials at select power outputs with targeted T_{lim} values of 2.5, 5, 10, and 13 min ($SVR_{2.5}$, SVR_5, SVR_{10}, and SVR_{13}, respectively). These power outputs were predicted from the computation of W'_{RAMP} retrieved from RCP_{CORR} and PO_{peak} (for details, see Data Analyses section).

Equipment and Data Collection

An electromagnetically braked cycle ergometer (Velotron; RacerMate, Seattle, WA) was used for all trials. Gas exchange and ventilatory variables were measured using a breath-by-breath metabolic cart (CPET; Cosmed, Rome, Italy). The system consisted of a turbine and a sampling line to measure, respectively, inspired and expired volumes and concentrations of gases. Before each test, the system was calibrated with a 3-L syringe and a gas mixture of known concentrations (16% O_2, 5% CO_2, balance N_2). Gas exchange and ventilatory data were scrutinized to remove any aberrant breaths not representative of the true physiological response and linearly interpolated on a second-by-second basis. The highest $\dot{V}O_2$ from the ramp-incremental test ($\dot{V}O_{2max}$) was computed from the highest 20-s rolling average. The $\dot{V}O_2$ elicited by RCP_{CORR} was computed by averaging the last 2 min before the 30th min. For the calculation of steady-state $\dot{V}O_2$ response, 2-min averages were also performed around the 20th min. The $[La^-]_b$ during the 30-min constant-load trials was assessed by drawing from a fingerpick a sample of capillary blood, which was immediately analyzed using a laboratory analyzer (Biosen C-Line; EKF Diagnostics, Barleben, Germany). For all rides, measures of $[La^-]_b$ at the time points of interest (i.e., 5th, 10th, 15th, 20th, 25th, and 30th min) were taken in triplicate, and the average of the two closest $[La^-]_b$ measures was used to establish the steady-state response.

Data Analyses

During rapidly incrementing ramp-tests, the relationship between $\dot{V}O_2$ and power output is misaligned by the incomplete expression of the $\dot{V}O_2$ kinetics. This misalignment begins immediately at ramp onset (20) and becomes progressively larger above GET (4). The two step transitions within the moderate- and heavy-intensity domains, performed, respectively, before and after the ramp-incremental phase, permits to retrospectively account for this misalignment and, thus, to identify the correct power outputs at GET and RCP (3). To this goal, a three-phase analysis was used as follows:

i) *Respiratory thresholds identification*. From the ramp-derived raw gas exchange and ventilatory variables, the $\dot{V}O_2$ values at GET and RCP were identified independently by two investigators, as previously described (6). In case of a disagreement, the two investigators would discuss their predictions together until a consensus was reached. Briefly, GET was determined as the point at which carbon dioxide production ($\dot{V}CO_2$) began to increase disproportionally with respect to $\dot{V}O_2$ (v-slope method). This point was corroborated by the identification of the first upward inflection point in the minute ventilation ($\dot{V}_E$) versus $\dot{V}O_2$ relationship coincidental with a leveling off in the end-tidal pressure of CO_2 ($P_{ET}CO_2$) (beginning of isocapnic buffering period) (21). By contrast, RCP was identified as the point at which $P_{ET}CO_2$ began to fall after the period of isocapnic buffering concomitantly with the second upward inflection point in $\dot{V}_E$ and $\dot{V}_E/\dot{V}CO_2$ versus $\dot{V}O_2$ relationships (22).

ii) *Moderate-intensity domain correction*. A linear regression was used to fit the ramp $\dot{V}O_2$ response from the onset of its systematic rise to the value estimated at GET. The steady-state $\dot{V}O_2$ during the moderate-intensity step transition was computed as the average of all breaths within the last 2 min. The difference between the ramp-derived power output extrapolated from the $\dot{V}O_2$ elicited by the step transition and the 80 W provided the "correction factor" (or mean response time [MRT]), which was calculated as follows:

$$\text{MRT (W)} = \left[\left(\dot{V}O_2 \text{ at 80 W} - \text{intercept}_{MOD}\right)/\text{slope}_{MOD}\right] - 80 \text{ W} \quad [1]$$

where intercept_{MOD} ($mL \cdot min^{-1}$) and slope_{MOD} ($mL \cdot min^{-1} \cdot W^{-1}$) are the parameters obtained from the linear regression of the ramp-derived $\dot{V}O_2$ response within the moderate-intensity domain. For each individual, the ramp-derived $\dot{V}O_2$ was "left-shifted" relative to the ramp power output by an amount equal to the MRT. This permitted the identification of the power output that would elicit, in steady state, the estimated $\dot{V}O_2$ at GET.

iii) *Heavy-intensity domain correction*. The steady-state $\dot{V}O_2$ during the heavy-intensity step transition after the ramp test was computed as the average of all breaths within the last 2 min. Thereafter, a linear regression from the $\dot{V}O_2$ and MRT-corrected power output at GET to the $\dot{V}O_2$ and power output of the heavy-intensity step transition was performed. The parameters of this linear regression were extrapolated to the value of $\dot{V}O_2$ at RCP and, by linear interpolation, the power output that would elicit, in steady state, the $\dot{V}O_2$ at RCP_{CORR}, was retrieved as follows:

$$RCP_{CORR} \text{ (W)} = \left(\dot{V}O_2 \text{ at RCP} - \text{intercept}_{HVY}\right)/\text{slope}_{HVY} \quad [2]$$

where intercept_{HVY} ($mL \cdot min^{-1}$) and slope_{HVY} ($mL \cdot min^{-1} \cdot W^{-1}$) are the parameters obtained from the linear regression between $\dot{V}O_2$ and power output at GET and at the heavy-intensity step transition.

Selecting the power output for $HVY_{50\%}$. The power output for the target heavy-intensity $\dot{V}O_2$ was retrieved via linear extrapolation of the $\dot{V}O_2$-to-power output relationship between GET and RCP. Specifically, the intercept_{HVY} and the slope_{HVY} parameters were used to retrieve via linear extrapolation the power output that would correspond to a $\dot{V}O_2$ value equidistant from

GET and RCP (50% of heavy-intensity domain; $HVY_{50\%}$). To compare targeted and measured $\dot{V}O_2$, the average of all breaths within the last 2 min was computed during $HVY_{50\%}$.

Selecting the power output for target T_{lim} within the severe-intensity domain. The relationship existing between constant-load power outputs and respective T_{lim} within the severe-intensity domain is well described by a hyperbolic function (23), whereby T_{lim} can be predicted as follows:

$$T_{lim} = W'/(P - CP) \quad [3]$$

where W' is the finite work capacity above CP (J), P is the selected power output (W), and CP (W) is the asymptote of the relationship. It has been previously demonstrated that the CP model can also be applied to ramp-incremental exercise (17), whereby T_{lim} during a ramp-incremental test can be predicted by a modified version of equation 3, as follows:

$$T_{lim} = CP/S + \sqrt{2}\, W'/S \quad [4]$$

where S is the rate of increase, or slope, of the ramp test (in the present study 0.5 $W \cdot s^{-1}$). With the SRS protocol, considering that the slope of the ramp test is known, T_{lim} is measured, and CP can be retrieved via RCP_{CORR} (10), by rearranging equation 4, we calculated each individual's ramp-derived W' (W'_{RAMP}) as follows:

$$T_{lim} = RCP_{CORR}/S + \sqrt{2}\, W'/S \quad [5]$$

Thereafter, by implementing RCP_{CORR} and W'_{RAMP} within equation 3, we selected for each individual four power outputs that would elicit tasks failure at the target durations of 2.5, 5, 10, and 13 min (i.e., $SVR_{2.5}$, SVR_5, SVR_{10}, and SVR_{13}, respectively). These target T_{lim} were chosen to confidently cover the widest possible range of severe-intensity power outputs, considering a possible measurement error between targeted and measured T_{lim} of ~10% (16). The performance of these trials was randomized, and each began after a 4-min, 20-W baseline.

CP modeling. By plotting the power outputs predicted for $SVR_{2.5}$, SVR_5, SVR_{10}, and SVR_{13} against T_{lim}, the CP model for each individual was derived using the following two-parameter models:

1. hyperbolic ($CP_{2\text{-}hyp}$):

$$T_{lim} = W'_{CONSTANT}/(P - CP) \quad [6]$$

2. linear work-time (CP_{lin}):

$$Work = CP \cdot T_{lim} + W'_{CONSTANT} \quad [7]$$

3. linear, inverse of time ($CP_{1/T_{lim}}$):

$$P = W'_{CONSTANT}\ (1/T_{lim}) + CP \quad [8]$$

The CP and the $W'_{CONSTANT}$ resulting from the model with the lowest combined standard error (SEE) (i.e., best model fit) were selected for subsequent comparisons with their analogous RCP_{CORR} and W'_{RAMP} (24). SEE was computed as $SEE(\hat{\beta}) = \frac{\hat{\beta}}{t}$, where β is calculated as the estimate and the t-value (t-value being the square root of the F-statistics).

Statistical Analyses

Data are presented as mean ± SD. Coefficients of variation (CV) are also presented where deemed necessary. Paired sample t-tests were used to compare the following: (i) the predicted and measured $\dot{V}O_2$ at RCP_{CORR}, (ii) the predicted and measured $\dot{V}O_2$ at $HVY_{50\%}$, (iii) the predicted and measured T_{lim} (min) of the severe-intensity constant-load trials, (iv) the power output at RCP_{CORR} and CP, and (v) the size (J) of W'_{RAMP} and $W'_{CONSTANT}$. Between variables, association was evaluated using Pearson's product–moment correlation, concordance using Lin's concordance coefficients (CCC), and agreement using biases and limits of agreement (LOA) calculated as part of Bland–Altman plots. The CCC was interpreted as follows: almost perfect concordance = CCC ≥ 0.99, substantial concordance = 0.99 < CCC ≥ 0.95, moderate concordance = 0.95 < CCC ≥ 0.90, and poor concordance = CCC < 0.90. Statistical significance was set at an α level < 0.05.

RESULTS

The group mean peak physiological responses recorded at the end of the ramp-incremental test are reported in Table 1. Results across all test visits for a representative participant are depicted in Figure 2.

SRS and RCP_{CORR} results. The steady state $\dot{V}O_2$ elicited by the 80-W moderate-intensity step transition preceding the ramp-incremental test was 1.47 ± 0.14 $L \cdot min^{-1}$. The MRT-derived correction to left-shift the $\dot{V}O_2$ data was 12 ± 7 W or 23 ± 15 s. The average power output used for the heavy-intensity step transition after the ramp-incremental test was 167 ± 42 W (or 51.9% ± 4.2% of PO_{peak}), which elicited a steady-state $\dot{V}O_2$ of 2.48 ± 0.52 $L \cdot min^{-1}$. From the ramp-incremental test, the $\dot{V}O_2$ values estimated at GET and RCP were, respectively, 1.99 ± 0.41 $L \cdot min^{-1}$ (59.6% ± 5.2% of $\dot{V}O_{2max}$) and 2.83 ± 0.65 $L \cdot min^{-1}$ (84.2% ± 4.0% of $\dot{V}O_{2max}$). The predicted power output at RCP_{CORR} was 192 ± 53 W (equating to 59.5% ± 6.1% of PO_{peak}). The steady-state $\dot{V}O_2$ measured during the 30-min constant-load trial at RCP_{CORR} was 2.85 ± 0.65 $L \cdot min^{-1}$ (or 84.8% ± 5.5% of $\dot{V}O_{2max}$) and was not different from the one estimated ($P = 0.72$). Furthermore, the predicted and measured $\dot{V}O_2$ at RCP_{CORR} demonstrated a strong correlation ($r = 0.98$), a substantial concordance (CCC = 0.98), and a high agreement

TABLE 1. Physiological responses derived from the ramp-incremental test.

N = 14 (5 Females)	
PO_{peak}, W	319 ± 64
PO_{peak}, $W \cdot kg^{-1}$	4.6 ± 0.8
$\dot{V}O_{2max}$, $L \cdot min^{-1}$	3.37 ± 0.78
$\dot{V}O_{2max}$, $mL \cdot kg^{-1} \cdot min^{-1}$	48.1 ± 8.8
HR_{max}, bpm	186 ± 7
$[La^-]_b$, mM	10.7 ± 1.8

Data are presented as mean ± SD.

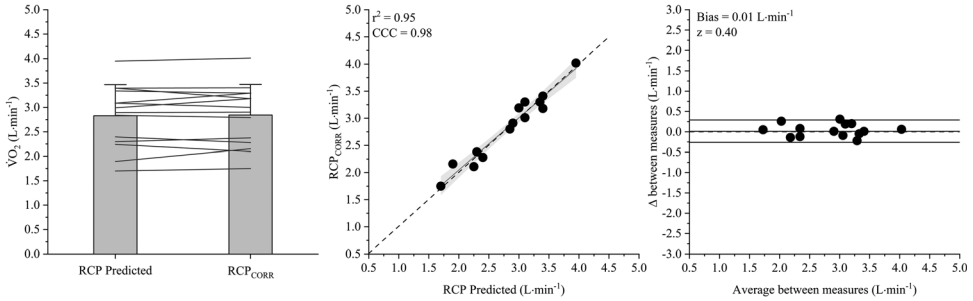

FIGURE 3—Group average, individual data, correlation, and Bland–Altman plots between predicted and measured $\dot{V}O_2$ at RCP_{CORR}.

(bias = 0.01 L·min^{-1}; LOA = −0.26 to 0.29 L·min^{-1}) between each other (Fig. 3). The $[La^-]_b$ values at baseline and at the 5th, 10th, 15th, 20th, 25th, and 30th min during the 30-min constant-load trial at RCP_{CORR} were, respectively, 1.4 ± 0.3, 4.8 ± 1.2, 5.8 ± 1.6, 6.1 ± 1.7, 6.4 ± 1.8, 6.7 ± 2.0, and 6.9 ± 2.3 mM. RCP_{CORR} elicited responses conforming to MMSS in all but two individuals. In these, steady-state physiological responses were still possible at 5% above RCP_{CORR}. For those in whom RCP_{CORR} corresponded to MMSS, exercise 5% above RCP_{CORR} was tolerable for 22.1 ± 6.6 min and culminated with a $\dot{V}O_2$ not different from $\dot{V}O_{2max}$ (3.28 ± 0.92 L·min^{-1}) (P = 0.171). The W'_{RAMP} from the CP model applied to the ramp test was 16388 ± 5040 J.

$HVY_{50\%}$ results. The target $\dot{V}O_2$ at $HVY_{50\%}$ was 2.41 ± 0.52 L·min^{-1}. From the SRS protocol, the $HVY_{50\%}$ power output identified to elicit this $\dot{V}O_2$ in steady state was 162 ± 43 W. At this power output, the measured $\dot{V}O_2$ was 2.43 ± 0.52 L·min^{-1}, which was not different from the targeted $\dot{V}O_2$ (P = 0.71). The CV between the targeted and the measured $\dot{V}O_2$ at $HVY_{50\%}$ was 4.0% ± 2.1%. Overall, between them, targeted and measured $\dot{V}O_2$ at $HVY_{50\%}$ demonstrated a strong correlation (r = 0.95), a substantial concordance (CCC = 0.95), and a high agreement (bias = 0.02 L·min^{-1}; LOA = −0.30 to 0.34 L·min^{-1}) (Fig. 4).

Severe-intensity trials results. From RCP_{CORR} and W'_{RAMP}, the power outputs for $SVR_{2.5}$, SVR_5, SVR_{10}, and SVR_{13} were, respectively, 302 ± 73, 247 ± 61, 219 ± 57, and 212 ± 55 W; the measured T_{lim} values for these power outputs were, respectively, 2.24 ± 0.53, 5.36 ± 0.74, 9.34 ± 1.60, and 13.04 ± 2.07 min. The targeted and the measured T_{lim} values were not different from each other (aggregate $P > 0.05$) (Fig. 5). From the shortest to the longest, the CV between targeted and measured T_{lim} were 15.1%, 8.7%, 10.5%, and 8.5%, respectively.

CP and W'_{CP} versus RCP_{CORR} and W'_{RAMP}. Of the three, two-parameter CP models, the "best model" fit (r^2 = 0.988 ± 0.013) corresponded to $CP_{2\text{-hyp}}$ in four participants, CP_{lin} in one participant, and CP_1/T_{lim} in the remaining nine participants. From these, the CP and the $W'_{CONSTANT}$ were 193 ± 53 W and 15810 ± 5494 J, whereas the aggregated SEE were 2.2% ± 1.6% and 8.6% ± 5.4%, respectively. The power output at CP and RCP_{CORR} were not different (P = 0.65) and demonstrated a strong correlation (r = 0.99), a high concordance (CCC = 0.99), and a high agreement (bias = 1 W; LOA = −14 to 16 W). Likewise, the work (J) corresponding with $W'_{CONSTANT}$ and W'_{RAMP} was not different (P = 0.51) and demonstrated a high correlation (r = 0.82), a high agreement (bias −578 J; LOA = −6801 to 5646 J), but poor concordance (CCC = 0.81) (Fig. 6).

DISCUSSION

With the ever-growing number of reports demonstrating the importance of individualizing the metabolic stimulus during exercise, it is paramount to develop strategies to prescribe exercise intensity in an accurate, simple, and time-efficient manner. To this aim, we recently developed and validated an SRS protocol (3), a methodology that combines the performance of one moderate- and one heavy-intensity step transition with a routine ramp-incremental test and allows prediction, within a single test visit, of the power outputs at LT and MMSS: the key, highly individual boundaries of exercise intensity. With the present study, we aimed to test the extended capabilities of the SRS protocol by testing its capacity to predict power outputs for target $\dot{V}O_2$ responses within the heavy-intensity domain and for discrete T_{lim} within the severe-intensity domain. In line with our hypotheses, findings

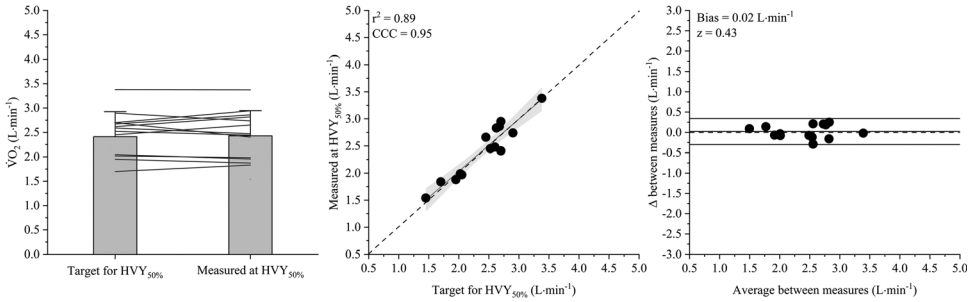

FIGURE 4—Group average, individual data, correlation, and Bland–Altman plots between predicted and measured $\dot{V}O_2$ at $HVY_{50\%}$.

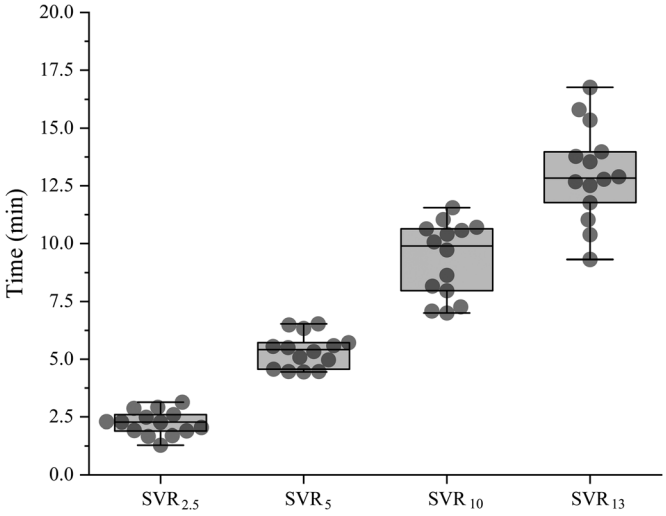

FIGURE 5—Group distribution of T_{lim} at the four identified power outputs to elicit exhaustion at minutes 2.5 ($SVR_{2.5}$), 5 (SVR_5), 10 (SVR_{10}), and 13 (SVR_{13}).

demonstrated that, for both goals, the SRS was highly accurate as the agreement between targeted and measured $\dot{V}O_2$ for $HVY_{50\%}$ was high, whereas the variance between targeted and measured severe T_{lim} was relatively small and in line with expected variability of severe-intensity exercise performance (16,25). In addition to this, RCP_{CORR} and W'_{RAMP} were not different from, and highly correlated with, their analogous CP and $W'_{CONSTANT}$. As such, our findings suggest that the SRS protocol can be used not only to predict with good accuracy LT and MMSS but also more broadly to predict power outputs to elicit tailored metabolic responses and exercise performances across the entire intensity spectrum.

Confirming the performance of the SRS protocol to identify LT and MMSS. A prerequisite to extend the predictive capabilities of the SRS protocol was to confirm that the ramp-derived RCP_{CORR} actually corresponded to MMSS. In line with our expectations, we found that RCP_{CORR} conformed to MMSS in the majority of the individuals (i.e., 12 of 14). In those in whom RCP_{CORR} incorrectly predicted MMSS, the highest metabolic steady state was observed at 5% above the power output at RCP_{CORR} (i.e., ~10 W), but metabolic stability was no longer possible another 5% above. Collectively, these outcomes, which agree with our original investigation (3), demonstrate the ability of the SRS protocol to produce estimates that fall rather consistently within the range of power outputs associated with MMSS. Even in circumstances where these estimates are incorrect, the error is on the order of a few watts (i.e., ~10 W) and, thus, well within the measurement and day-to-day variability of the responses under investigation.

Predicting the power output for a target heavy-intensity metabolic rate. A tenet of the SRS protocol is that the increase in the gain of $\dot{V}O_2$ between GET and RCP

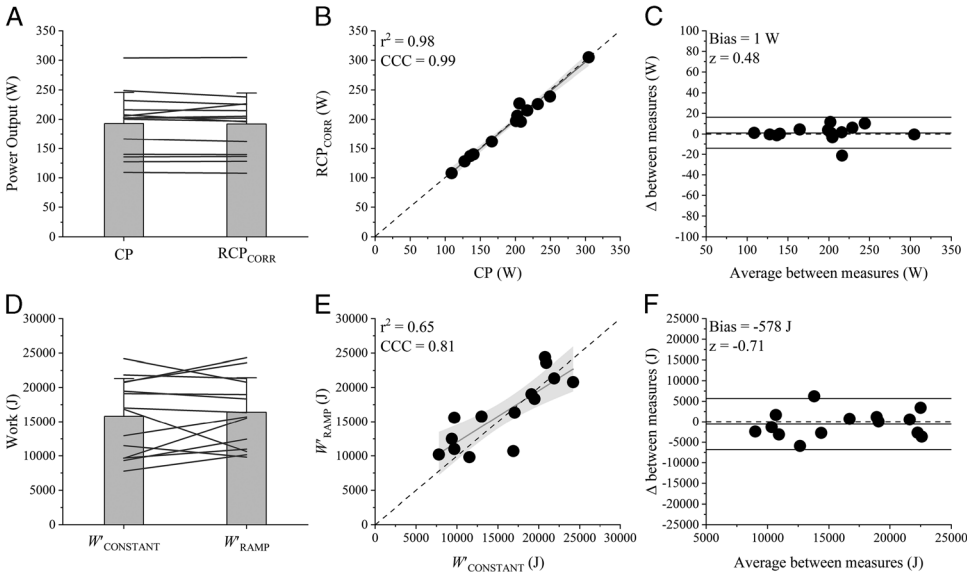

FIGURE 6—Comparisons (A and D), correlations (B and E) and agreement between CP and RCP_{corr} and between $W'_{constant}$ and W'_{ramp}.

is linear (3). Thus, once both the $\dot{V}O_2$ and the power output at these indices are estimated via the SRS protocol, such linearity suggests the possibility of retrieving via linear interpolation any power output eliciting a target steady-state $\dot{V}O_2$ within the heavy-intensity domain. To test this possibility, we targeted a $\dot{V}O_2$ equidistant from GET and RCP hypothesizing that if indeed changes in $\dot{V}O_2$ gain are linear, then targeted and measured $\dot{V}O_2$ at the extrapolated power output (i.e., $HVY_{50\%}$) should not be different from each other. In line with this hypothesis, we found that the measured $\dot{V}O_2$ response at $HVY_{50\%}$ was not different from and substantially concordant with the targeted $\dot{V}O_2$ (Fig. 4). Specifically, the group mean bias of measured versus targeted $\dot{V}O_2$ was ~20 $mL \cdot min^{-1}$, whereas the CV was ~4% (or ~40 $mL \cdot min^{-1}$). Considering that the average noise/variability of $\dot{V}O_2$ for a given power output is on the order of 120 $mL \cdot min^{-1}$ (26), these results highlight the high accuracy by which the SRS protocol can elicit a target metabolic rate within the heavy-intensity domain.

Predicting the power output for discrete T_{lim} within the severe-intensity domain and comparison between CP and RCP_{CORR} and between $W'_{CONSTANT}$ and W'_{RAMP}. According to the CP construct (23), well-motivated individuals fail a severe-intensity constant-load task when W' is fully depleted. Interestingly, although presenting some variability (15), the size of W' remains fairly consistent across different exercise paradigms, such self-paced (24), all-out (27), and ramped exercise (16). Such a remarkable constancy derives from the fact that, for exercise within the severe-intensity domain, muscular work relies substantially on anaerobic energy sources, which progressive depletion leads to the attainment of a consistent level of metabolic perturbations (28) impairing the ability of the individual to sustain the imposed power output (29), or any power output >CP (30).

For ramp-incremental exercise, W' (i.e., W'_{RAMP}) can be mathematically retrieved with knowledge of the incrementing rate used, PO_{peak} attained, and the individual's CP (17). Considering that for the SRS protocol the ramp rate is known by design, PO_{peak} is measured, and CP can be assumed to correspond to RCP_{CORR}, we hypothesized that the performance of this protocol would enable the computation of W'_{RAMP} and, thus, permit the prediction of discrete power outputs to elicit target T_{lim} within the severe-intensity domain. To test this hypothesis, we targeted T_{lim} of 2.5, 5, 10, and 13 min, and following our expectations, it was found that the identified power outputs elicited T_{lim} that were not different from the targeted ones with an aggregated variability (i.e., CV) between the measured and the targeted T_{lim} of approximately 10% (Fig. 5).

To further corroborate the predictive ability of the SRS protocol, we used the four severe-intensity constant-load trials to calculate CP and W' (i.e., $W'_{CONSTANT}$), and we compared these to their analogous SRS-derived RCP_{CORR} and W'_{RAMP}. Notably, CP and RCP_{CORR} were not different from each other, with bias being remarkably low and concordance approaching 1.0 (Fig. 6) indicating that, in healthy individuals, RCP_{CORR} may be used as a valid surrogate of CP and, thus, MMSS. By contrast, although not different and strongly correlated, $W'_{CONSTANT}$ and W'_{RAMP} were characterized by a relatively greater bias and lower concordance levels compared with what was observed between CP and RCP_{CORR} (Fig. 6). In this context, considering the similarity between CP and RCP_{CORR}, it is safe to say that most of the variability between predicted and targeted T_{lim} might have been due to some error in the quantifications of W'_{RAMP}. In this regard, potential sources of error can arise from day-to-day variations in performance during ramp-incremental tests, typically reported to be around 5% (31,32). In addition to this, CP and W' have also been demonstrated to be sensitive to manipulations of $\dot{V}O_2$ kinetics (33,34), which expression differs between square-wave transitions and ramp-incremental tests (5). Indeed, for square-wave transitions within the severe-intensity domain, the $\dot{V}O_2$ response demonstrates a slow rising component that adds onto the fundamental phase of $\dot{V}O_2$ kinetics as the expression of a greater O_2 cost of the exercise (2). Notably, the magnitude of such slow component and the size of W' are strongly related (35). However, because during rapidly incrementing ramp tests its development is obscured by the continuous increase in power output (5), it cannot be excluded that these discrete $\dot{V}O_2$ kinetics manifestations could influence the relationship between the constant-load- and the SRS-derived W'. Finally, there is evidence suggesting that supra-MMSS exercise performance is determined not only by the amount of W' remaining but also by its rate of utilization (16). For instance, during extreme-intensity exercise, the total amount of work accruable above MMSS is markedly smaller than $W'_{CONSTANT}$ (36), which is consistent with the presence of some limitation to exploit the remaining amount of W' at this very high rate of ATP turnover. Given that rapidly incrementing ramp-tests generally end within the extreme-intensity domain (37), the presence of such limitation cannot be ruled out and, thus, could represent a source of error when estimating W'_{RAMP}. In this regard, Black et al. (15) observed that CP and $W'_{CONSTANT}$ overestimate T_{lim} (i.e., PO_{peak}) during a ramp-incremental test by approximately 3% (or ~11 W). Recently, Caen et al. (38) reported a similar finding, whereby W' was greater (~10%) when derived from constant-load severe-intensity trials as compared with a ramp-incremental test. However, it is important to restate that, within the present dataset, RCP_{CORR} and W'_{RAMP} were not different from their analogous CP and $W'_{CONSTANT}$. Consequently, when using the latter two to retrospectively predict T_{lim} during the ramp-incremental test (as done previously (15)), predicted and measured ramp T_{lim} in our dataset are not different (i.e., 634 ± 132 vs 637 ± 127 s). This finding corroborates our underlying assumption that CP and $W'_{CONSTANT}$ can be derived from a ramp-incremental test. In this context, putative reasons for these somewhat contrasting findings could be related to the influence of the number of severe-intensity trials used to determine CP and $W'_{CONSTANT}$, the use of a fixed heavy-intensity $\dot{V}O_2$ gain to derive RCP_{CORR} across all participants, and/or employment of different ramp slopes. Nonetheless, it must be recognized that in all these studies, including the present, the magnitude of the intraindividual variability between W'_{RAMP} and $W'_{CONSTANT}$ and/or the predicted and measured T_{lim} during the ramp-incremental test or constant-load

severe-intensity trials are within the expected day-to-day performance variability for high intensity exercise (e.g., ~10%) (25,39). Therefore, in our opinion, that the RCP_{CORR} could be substituted for CP to derive an accurate estimate of W' and predict, with good accuracy, a range of T_{lim} within the severe-intensity domain provides evidence to synonymity of RCP with CP and its surrogacy for the MMSS (6).

Strengths and applicability of the SRS protocol. Of the several methods developed over the years to prescribe intensity of exercise, none possesses the advantages of the SRS protocol. Indeed, as demonstrated herein, this protocol has the ability to retrieve the power output for any target metabolic rate for which a steady-state response is attainable (i.e., moderate- and heavy-intensity domain) or any T_{lim} where exercise performance is delimited by the hyperbolic relationship existing between power outputs and duration for which they can be tolerated and where exercise culminates with attainment of $\dot{V}O_{2max}$ (i.e., severe-intensity domain). More broadly, with the SRS, one can retrieve with reasonable accuracy all aerobic parameters (i.e., LT, MMSS, W', and $\dot{V}O_{2max}$) that are essential for a comprehensive physiological characterization of individuals, for performance prediction, and for an appropriate prescription of exercise intensity. Compared with other methodologies that are less time efficient and/or necessitate inclusion of a series of maximal efforts, the SRS protocol requires only a single laboratory visit and a single maximal effort. Granted access to a metabolic cart for the measurement of gas exchange and ventilatory variables, such features make the SRS protocol potentially implementable in all settings ranging from sports performance to clinical.

Methodological considerations, limitations, and ongoing debates. For the SRS protocol to provide accurate estimations, measurements of the variables included in the computation of the power output at GET/LT and RCP/MMSS must be performed with a high degree of accuracy. In this context, all available plots should be used in combination to optimize detection of the $\dot{V}O_2$ at GET and RCP (6). Furthermore, as is the case for other approaches, an accurate estimation of W' relies on a fully exhaustive effort of the participants during the ramp-incremental exercise. We recognize that this might be more difficult to obtain in individuals unfamiliar with the testing procedures. In this context, although theoretically implementable in most clinical settings, future studies are warranted to confirm whether the SRS can be used reliably within populations who might (i) have impaired ability to exercise hard enough to achieve/develop a respiratory compensation, (ii) present with abnormal breathing patterns and respiratory constraints, and/or (iii) be under medication that could alter their chemoreflex responsiveness (14,40,41). In all these circumstances, the identification of GET and RCP may be more challenging and could, thus, limit the applicability of the SRS protocol.

Also linked to these aspects, there continues to be debate as to whether the RCP can be used as a proxy of MMSS. Most of this debate is based on the notion that rather than built on a metabolic construct (which would support a metabolic link between RCP and MMSS), the RCP represents the expression of a "ventilatory control," which kinetics is dependent on some amplitude and/or time-related threshold for H^+ sensing by the carotid chemoreceptors (42). Support to this view resides within the evidence that the kinetics of $\dot{V}O_2$ and minute ventilation are different (43) and the onset of the respiratory compensation in terms of its associated power output occurs progressively closer to GET the slower the ramp incrementing rate (4). What, however, is often underappreciated is that the $\dot{V}O_2$ at which such compensatory response is initiated remains remarkably similar no matter the rate of the forcing function (4,9,44), which suggests, on the contrary, that it might be the trespassing of a "critical" metabolic rate that promotes the chemoreflex-mediated response underpinning the manifestation of RCP. This might be because, independent of the ventilatory output at the $\dot{V}O_2$ of RCP, the cascade of events (transduction and circulatory times of metabolic signaling from muscle to blood and to carotid bodies; neurally mediated reflex response) leading to the hyperventilation occurs very rapidly (45–47). In our opinion, the close agreement between RCP_{CORR} and CP (and thus MMSS) herein seems to only reinforce our view.

CONCLUSIONS

In summary, in this study, we have tested the extended capabilities of the previously developed SRS protocol (3). Specifically, we demonstrated that the use of this protocol can aid with the prediction of power outputs to elicit targeted metabolic rates within the heavy-intensity domain and, although with some degree of variability, discrete exercise durations within the severe-intensity domain. Such unique features make the SRS protocol suitable to individualize the metabolic stimulus of exercise across the entire intensity spectrum.

This study was supported by grants given to Juan M. Murias by the Natural Sciences and Engineering Research Council of Canada (RGPIN-2016-03698) and the Heart and Stroke Foundation of Canada (1047725). No conflicts of interest, financial or otherwise, are declared by the authors. The results of the study are presented clearly, honestly, and without fabrication, falsification, or inappropriate data manipulation. The results of the present study do not constitute endorsement by the American College of Sports Medicine.

REFERENCES

1. Whipp BJ. Domains of aerobic function and their limiting parameters. In: *The Physiology and Pathophysiology of Exercise Tolerance*. Boston (MA): Springer; 1996. pp. 83–9.
2. Rossiter HB. Exercise: kinetic considerations for gas exchange. *Compr Physiol*. 2011;1(1):203–44.
3. Iannetta D, Inglis EC, Pogliaghi S, Murias JM, Keir DA. A "step–ramp–step" protocol to identify the maximal metabolic steady state. *Med Sci Sports Exerc*. 2020;52(9):2011–9.
4. Iannetta D, de Almeida Azevedo R, Keir DA, Murias JM. Establishing the $\dot{V}O_2$ versus constant-work-rate relationship from ramp-incremental exercise: simple strategies for an unsolved problem. *J Appl Physiol (1985)*. 2019;127(6):1519–27.
5. Keir DA, Benson AP, Love LK, Robertson TC, Rossiter HB, Kowalchuk JM. Influence of muscle metabolic heterogeneity in determining the $\dot{V}O2p$ kinetic response to ramp-incremental exercise. *J Appl Physiol (1985)*. 2016;120(5):503–13.

6. Keir DA, Iannetta D, Mattioni Maturana F, Kowalchuk JM, Murias JM. Identification of non-invasive exercise thresholds: methods, strategies, and an online app. *Sports Med*. 2022;52(2):237–55.
7. Broxterman RM, Craig JC, Richardson RS. The respiratory compensation point and the deoxygenation break point are not valid surrogates for critical power and maximum lactate steady state. *Med Sci Sports Exerc*. 2018;50(11):2379–82.
8. Broxterman RM, Ade CJ, Craig JC, Wilcox SL, Schlup SJ, Barstow TJ. The relationship between critical speed and the respiratory compensation point: coincidence or equivalence. *Eur J Sport Sci*. 2015;15(7):631–9.
9. Leo JA, Sabapathy S, Simmonds MJ, Cross TJ. The respiratory compensation point is not a valid surrogate for critical power. *Med Sci Sports Exerc*. 2017;49(7):1452–60.
10. Keir DA, Fontana FY, Robertson TC, et al. Exercise intensity thresholds: identifying the boundaries of sustainable performance. *Med Sci Sports Exerc*. 2015;47(9):1932–40.
11. Keir DA, Pogliaghi S, Murias JM. The respiratory compensation point and the deoxygenation break point are valid surrogates for critical power and maximum lactate steady state. *Med Sci Sports Exerc*. 2018;50(11):2375–8.
12. Caen K, Vermeire K, Bourgois JG, Boone J. Exercise thresholds on trial: are they really equivalent? *Med Sci Sports Exerc*. 2018;50(6):1277–84.
13. Keir DA, Mattioni Maturana F, Iannetta D, Murias JM. Comment on: "relative proximity of critical power and metabolic/ventilatory thresholds: systematic review and meta-analysis." *Sports Med*. 2021;51(2):367–8.
14. Tiller NB, Porszasz J, Casaburi R, Rossiter HB, Ferguson C. Critical power and respiratory compensation point are not equivalent in patients with COPD. *Med Sci Sports Exerc*. 2023;55(6):1097–104.
15. Black MI, Jones AM, Kelly JA, Bailey SJ, Vanhatalo A. The constant work rate critical power protocol overestimates ramp incremental exercise performance. *Eur J Appl Physiol*. 2016;116(11–12):2415–22.
16. Chidnok W, Dimenna FJ, Bailey SJ, Wilkerson DP, Vanhatalo A, Jones AM. Effects of pacing strategy on work done above critical power during high-intensity exercise. *Med Sci Sports Exerc*. 2013;45(7):1377–85.
17. Morton RH. Critical power test for ramp exercise. *Eur J Appl Physiol Occup Physiol*. 1994;69(5):435–8.
18. Iannetta D, Inglis EC, Mattu AT, et al. A critical evaluation of current methods for exercise prescription in women and men. *Med Sci Sports Exerc*. 2020;52(2):466–73.
19. Iannetta D, Ingram CP, Keir DA, Murias JM. Methodological reconciliation of CP and MLSS and their agreement with the maximal metabolic steady state. *Med Sci Sports Exerc*. 2022;54(4):622–32.
20. Iannetta D, Murias JM, Keir DA. A simple method to quantify the $\dot{V}O_2$ mean response time of ramp-incremental exercise. *Med Sci Sports Exerc*. 2019;51(5):1080–6.
21. Beaver WL, Wasserman K, Whipp BJ. A new method for detecting anaerobic threshold by gas exchange. *J Appl Physiol (1985)*. 1986; 60(6):2020–7.
22. Whipp BJ, Davis JA, Wasserman K. Ventilatory control of the 'isocapnic buffering' region in rapidly-incremental exercise. *Respir Physiol*. 1989;76(3):357–67.
23. Monod H, Scherrer J. The work capacity of a synergic muscular group. *Ergonomics*. 1965;8(3):329–38.
24. Black MI, Jones AM, Bailey SJ, Vanhatalo A. Self-pacing increases critical power and improves performance during severe-intensity exercise. *Appl Physiol Nutr Metab*. 2015;40(7):662–70.
25. McLellan TM, Cheung SS, Jacobs I. Variability of time to exhaustion during submaximal exercise. *Can J Appl Physiol*. 1995;20(1):39–51.
26. Keir DA, Murias JM, Paterson DH, Kowalchuk JM. Breath-by-breath pulmonary O_2 uptake kinetics: effect of data processing on confidence in estimating model parameters. *Exp Physiol*. 2014;99(11):1511–22.
27. Vanhatalo A, Doust JH, Burnley M. Determination of critical power using a 3-min all-out cycling test. *Med Sci Sports Exerc*. 2007;39(3):548–55.
28. Black MI, Jones AM, Blackwell JR, et al. Muscle metabolic and neuromuscular determinants of fatigue during cycling in different exercise intensity domains. *J Appl Physiol (1985)*. 2017;122(3):446–59.
29. Fukuba Y, Miura A, Endo M, Kan A, Yanagawa K, Whipp BJ. The curvature constant parameter of the power–duration curve for varied-power exercise. *Med Sci Sports Exerc*. 2003;35(8):1413–8.
30. Coats EM, Rossiter HB, Day JR, Miura A, Fukuba Y, Whipp BJ. Intensity-dependent tolerance to exercise after attaining V(O2) max in humans. *J Appl Physiol (1985)*. 2003;95(2):483–90.
31. Zinner C, Gerspitzer A, Düking P, et al. The magnitude and time-course of physiological responses to 9 weeks of incremental ramp testing. *Scand J Med Sci Sports*. 2023;33(7):1146–56.
32. Weston SB, Gabbett TJ. Reproducibility of ventilation of thresholds in trained cyclists during ramp cycle exercise. *J Sci Med Sport*. 2001; 4(3):357–66.
33. Burnley M, Davison G, Baker JR. Effects of priming exercise on $\dot{V}O_2$ kinetics and the power–duration relationship. *Med Sci Sports Exerc*. 2011;43(11):2171–9.
34. Goulding RP, Roche DM, Marwood S. Effect of hyperoxia on critical power and $\dot{V}O_2$ kinetics during upright cycling. *Med Sci Sports Exerc*. 2020;52(5):1041–9.
35. Murgatroyd SR, Ferguson C, Ward SA, Whipp BJ, Rossiter HB. Pulmonary O_2 uptake kinetics as a determinant of high-intensity exercise tolerance in humans. *J Appl Physiol (1985)*. 2011;110(6):1598–606.
36. Iannetta D, Zhang J, Murias JM, Aboodarda SJ. Neuromuscular and perceptual mechanisms of fatigue accompanying task failure in response to moderate-, heavy-, severe-, and extreme-intensity cycling. *J Appl Physiol (1985)*. 2022;133(2):323–34.
37. Iannetta D, de Almeida Azevedo R, Ingram CP, Keir DA, Murias JM. Evaluating the suitability of supra-PO_{peak} verification trials after ramp-incremental exercise to confirm the attainment of maximum O_2 uptake. *Am J Physiol Regul Integr Comp Physiol*. 2020;319(3):R315–22.
38. Caen K, Bourgois JG, Stuer L, Mermans V, Boone J. Can we accurately predict critical power and *W′* from a single ramp incremental exercise test? *Med Sci Sports Exerc*. 2023;55(8):1401–8.
39. Barbosa LF, Montagnana L, Denadai BS, Greco CC. Reliability of cardiorespiratory parameters during cycling exercise performed at the severe domain in active individuals. *J Strength Cond Res*. 2014; 28(4):976–81.
40. Carriere C, Corrà U, Piepoli M, et al. Anaerobic threshold and respiratory compensation point identification during cardiopulmonary exercise tests in chronic heart failure. *Chest*. 2019;156(2):338–47.
41. Rovai S, Contini M, Sciomer S, Vignati C, Agostoni P. The double anaerobic threshold in heart failure. *Int J Cardiol*. 2022;353:68–70.
42. Ward SA. Exercise physiology: exercise hyperpnea. *Curr Opin Physiol*. 2019;10:166–72.
43. Casaburi R, Barstow TJ, Robinson T, Wasserman K. Influence of work rate on ventilatory and gas exchange kinetics. *J Appl Physiol (1985)*. 2017;67(2):547–55.
44. Scheuermann BW, Kowalchuk JM. Attenuated respiratory compensation during rapidly incremented ramp exercise. *Respir Physiol*. 1998;114(3):227–38.
45. Austin C, Wray S. Extracellular pH signals affect rat vascular tone by rapid transduction into intracellular pH changes. *J Physiol*. 1993;466:1–8.
46. Rigatto M, Jones NL, Campbell EJ. Pulmonary recirculation time: influence of posture and exercise. *Clin Sci*. 1968;35(2):183–95.
47. Gonzalez C, Almaraz L, Obeso A, Rigual R. Carotid body chemoreceptors: from natural stimuli to sensory discharges. *Physiol Rev*. 1994;74(4):829–98.